Connectivity effects in the dynamic model of neural networks

2009 J. Phys. A: Math. Theor. 42 205003

(http://iopscience.iop.org/1751-8121/42/20/205003)

IOP PUBLISHING JOURNAL OF PHYSICS A: MATHEMATICAL AND THEORETICAL

J. Phys. A: Math. Theor. **42** (2009) 205003 (9pp) doi:10.1088/1751-8113/42/20/205003

Connectivity effects in the dynamic model of neural networks

J Choi[1], **M Y Choi**[2] **and B-G Yoon**[3,4,5]

[1] Department of Physics and Department of Chemical Engineering, Keimyung University, Daegu 704-701, Korea
[2] Department of Physics and Astronomy and Center for Theoretical Physics, Seoul National University, Seoul 151-747, Korea
[3] Department of Physics, University of Ulsan, Ulsan 680-749, Korea
[4] Research Center for Dielectric and Advanced Material Physics, Pusan National University, Busan 609-735, Korea

E-mail: bgyoon@ulsan.ac.kr

Received 6 February 2009, in final form 1 April 2009
Published 30 April 2009
Online at stacks.iop.org/JPhysA/42/205003

Abstract

We study, via extensive Monte Carlo calculations, the effects of connectivity in the dynamic model of neural networks, to observe that the Mattis-state order parameter increases with the number of coupled neurons. Such effects appear more pronounced when the average number of connections is increased by introducing shortcuts in the network. In particular, the power spectra of the order parameter at stationarity are found to exhibit power-law behavior, depending on how the average number of connections is increased. The cluster size distribution of the 'memory-unmatched' sites also follows a power law and possesses strong correlations with the power spectra. It is further observed that the distribution of waiting times for neuron firing fits roughly to a power law, again depending on how neuronal connections are increased.

PACS numbers: 05.65.+b, 87.18.Bb, 87.18.Sn

1. Introduction

Many biological systems in diverse areas apparently exhibit no characteristic scale spatially and/or temporally, manifested by power-law distributions of the event sizes and durations in the dynamics [1]. Numerous evidences can be found particularly in brain activity: for instance, an electroencephalogram displays $1/f$ frequency scaling [2] and wait times (interspike intervals) in cortex neurons follow a power-law distribution [3]. Such scale invariance properties are

[5] Author to whom any correspondence should be addressed.

often referred to as originating from spatio-temporal correlations among their constituents [4] and regarded as a footprint of the so-called self-organized criticality (SOC) [5, 6].

On the other hand, there is experimental evidence [7, 8] that some regions of the nervous system, e.g., the visual cortex, possess small-world geometry [9]. It is well known that neural networks in small-world topology have many advantages: memory retrieval performance is enhanced as compared to random-network topology with the same total connection length [10]. Likewise the connection topology is expected to affect the dynamics of the system substantially. There is, however, little work addressing dynamics of the neural network on the small-world geometry [11], and it is of interest to probe how the dynamic properties change, depending upon the small-world topology.

For this purpose we adopt a dynamic model for neural networks, which uses continuous time and takes explicitly into account several time scales such as the refractory period, time duration of the action potential and the retardation of signal propagation [12]. These dynamic characteristics are realistic in view of the biological situation and seemingly encompass the necessary ingredients of the SOC-type dynamics, accumulation and dissipation of energy. With a simple Hebb-type rule [13], the model reproduces desirable features similar to those of conventional models [14, 15] in the fully connected limit. The model has further been extended to the cases in which neuronal loss proceeds, incorporated with the dynamic failure model [16]. In a related dynamic failure model for biological systems, it has been found that both temporal and spatial correlations are correlated, exhibiting power-law behavior, which is attributed to the interplay of the phase transition and SOC [17].

In this work, we study the connectivity effects in the neural network, focusing on the (global) order parameter and on the dynamic properties of the system. The connectivity is varied in two ways, either by increasing the number of coupled neighbors or by introducing shortcuts between neurons. It is observed that the order parameter in general grows with the number of connections, as expected. We then compute the power spectrum of the order parameter, which exhibits, for a given value of the order parameter, different shapes depending on how the connectivity is varied. Further, the power spectrum has correlations with the cluster size distribution of memory-unmatched neurons; both exhibit power-law behavior. We also consider the wait time, i.e., the time elapse for a neuron to wait for the next firing, and find its distribution to follow roughly a power law.

This paper consists of four sections. In section 2, the dynamic model of neural networks is described, together with the method of Monte Carlo (MC) calculations. Section 3 presents the results of MC calculations, describing the connectivity effects of the network. Finally, a summary is given in section 4.

2. Dynamic model and Monte Carlo calculations

We consider a neural network consisting of N neurons, the ith of which is modeled by an Ising spin $s_i = \pm 1$. The threshold behavior of the ith neuron at time t is described by a probability that depends on the local potential

$$E_i(t - t_d) = \sum_j J_{ij}(t - t_d)s_j(t - t_d), \tag{1}$$

where $2J_{ij}$ is the strength of the synaptic junction from the jth neuron to the ith one ($J_{ii} = 0$) and $s_j(t - t_d)$ denotes the state of the jth neuron at time $t - t_d$ with t_d being the time delay in interaction (i.e., retardation of signal propagation, mostly through the synaptic junction) [12].

According to the simple Hebb-type learning rule [13], the synaptic strength is constructed of p stored patterns

$$J_{ij} = \begin{cases} N^{-1}\sum_{\mu=1}^{p}\sigma_i^\mu\sigma_j^\mu & \text{for} \quad i \neq j \\ 0 & \text{for} \quad i = j, \end{cases} \tag{2}$$

where $\sigma_i^\mu = \pm 1$ is the state of the ith neuron in pattern $\mu(=1, 2, \ldots, p)$.

We first prescribe the conditional probability that the ith neuron fires at time $t + \delta t$ given that it does not fire at time t

$$p(s_i = +1, t + \delta t | s_i = -1, t; \mathbf{s}', t - t_d) = \frac{\delta t}{2t_r}[1 + \tanh\beta E_i'], \tag{3}$$

where $\mathbf{s}' \equiv (s_1', s_2', \ldots, s_N')$ represents the configuration of the system at time $t - t_d$ and the 'temperature' $T \equiv 1/\beta$ measures the width of the threshold region or the noise level. Except for the factor $(2t_r)^{-1}\delta t$, which takes into account the existence of the refractory period t_r, the above expression has been chosen essentially following [14]. Similarly, we write the conditional probability that the ith neuron does not fire at time $t + \delta t$ given that it fires at time t. For sufficiently small δt, the probability on the average over all the neurons may be written in the form

$$p(s_i = -1, t + \delta t | s_i = +1, t; \mathbf{s}', t - t_d) = \frac{\delta t}{t_0}, \tag{4}$$

where t_0 is the time duration of the action potential, usually of the order of one to a few milliseconds. Thus the time average has been essentially incorporated in the above expression.

After rescaling time t in units of the delay time t_d, equations (3) and (4) can be combined to give an expression for the conditional probability $p(-s_i, t + \delta t | s_i, t; \mathbf{s}', t - t_d)$, which, in the limit $\delta t \to 0$, can be expressed in terms of the transition rate:

$$p(-s_i, t + \delta t | s_i, t; \mathbf{s}', t - 1) = w_i(s_i; \mathbf{s}', t - 1)\delta t. \tag{5}$$

The transition rate is given by

$$w_i(s_i; \mathbf{s}', t - 1) = \frac{1}{2\tau}\left[\left(a + \frac{1}{2}\right) + \left(a - \frac{1}{2}\right)s_i + \frac{1 - s_i}{2}\tanh\beta E_i'\right], \tag{6}$$

with $a \equiv t_r/t_0$ and $\tau \equiv t_r/t_d$.

The behavior of the network is then governed by the master equation, which describes the evolution of the joint probability $P(\mathbf{s}, t; \mathbf{s}', t - 1)$ that the system is in state $\mathbf{s}'$ at time $t - 1$ and in state $\mathbf{s}$ at time t. In consequence, equations describing the time evolution of relevant physical quantities, with the average taken over $P(\mathbf{s}, t; \mathbf{s}', t - 1)$, in general assume the form of differential-difference equations due to the delay in interactions. For example, one may find the equation of motion for the activity of the ith neuron, $m_i(t) \equiv \langle s_i \rangle_t \equiv \sum_{\mathbf{s}}\sum_{\mathbf{s}'} s_i P(\mathbf{s}, t; \mathbf{s}', t-1)$, which, in the case of the infinite-range interaction or in the fully connected limit, leads to the self-consistency equation [12]. One may also find the time evolution equation for the 'order parameter' $q^\mu(t) \equiv N^{-1}\sum_i \sigma_i^\mu m_i(t)$, which describes the overlap between the neurons and the memory μ.

In this work, we focus on the Mattis-state solution of the form $q^\mu(t) \equiv q(t)\delta_{\mu 1}$, which is fully correlated with just one of the quenched memories. As usual, patterns are generated at random, i.e., σ_i^μ is taken to be a quenched random variable, assuming $+1$ and -1 with equal probabilities:

$$p(\sigma_i^\mu) = \tfrac{1}{2}\delta(\sigma_i^\mu - 1) + \tfrac{1}{2}\delta(\sigma_i^\mu + 1). \tag{7}$$

To investigate the connectivity effects, we put neurons on a square lattice of linear size L and perform dynamic MC calculations with the transition rate in equation (6), varying the

number of coupled neurons or the number of connections per neuron. We increase the number of connections in two ways: (i) For each neuron we increase the number of coupled neurons up to nth nearest neighbors. In this way a particular neuron becomes coupled with k_0 other neurons. (ii) Another way to increase the number of neurons is to construct a small-world network, starting from the $L \times L$ square lattice and adding a shortcut with given probability between each neuron and another chosen randomly [18]. To this end, we fix the coupling within the nearest or the next nearest neighbors (setting $k_0 = 8$) and probe the behavior of the system as $N_{\rm sc}$, the total number of shortcuts, is varied. Obviously, only connected neurons can interact, so that J_{ij} in equation (2) does not vanish only if the ith neuron and the jth one are connected with each other.

In MC calculations, we use the lattice size $L = 64$ and 128 with up to five memory patterns ($1 \leqslant p \leqslant 5$), which are generated according to equation (7) at each run. The initial state of the system is chosen to be one of the memories, which, together with the p memories and given connectivity of the lattice, comprises one configuration. Specifically, we consider 30–100 different configurations for each set of values (a, T) and set the relaxation time $\tau = 5$ and the time step $\Delta t = 0.5$. These parameter values have been varied, only to give no appreciable difference except for the time scale. Then the neuronal states are allowed to flip according to the transition probabilities in equations (3) and (4). Among ordered states of the system, we choose only the Mattis state. Behaviors of the order parameters and other results described below do not depend qualitatively on the number p of memory patterns examined ($1 \leqslant p \leqslant 5$), and here only the results for $p = 2$ are presented. We presume that those behaviors persist qualitatively unchanged even for larger values of $p(\ll N)$, provided that the Mattis state exists unambiguously, although we have not considered fully such large values. For large values of p, the ordered Mattis state is observed very rarely during simulations, especially in the parameter regime where the order–disorder transition takes place. Accordingly, it takes an enormous amount of computing time to probe the system.

3. Results

Figure 1 displays the Mattis-state order parameter $\bar{q}$ averaged over time versus k, the average number of connections per neuron, obtained from MC calculations for a system of $N = 4096$ neurons with the time ratio $a = 0.5$, on a square lattice of size $L = 64$ at temperature $T = 0.1$. Only the data points for the ordered stationary state are plotted; in the region where there are no data points we have $\bar{q} = 0$. In the case that k_0 is raised by just increasing the number of nearest neighbors (solid circles), $\bar{q}$ grows slowly with k, approaching the mean-field value $\bar{q}^{MF} = 0.66$ at $k \approx 45$. On the other hand, when shortcuts are introduced with fixed $k_0(=8)$ (empty circles), the growth is more rapid and saturation is reached at a relatively smaller value of $k(\approx 20)$. This manifests that the presence of shortcuts in the system, allowing a neuron to couple to other neurons far apart, makes the system more mean-field-like than just increasing the number of coupled neurons. Such performance is one of the well-known features of the small-world network [9]. As addressed, the behavior displayed in figure 1 remains qualitatively the same even if p is increased (data not shown). However, in order to achieve the same value of the order parameter $\bar{q}$, we need more connections, i.e., larger values of k, as p is increased.

In figure 2, we present the power spectrum $P(\omega)$ of the order parameter $q(t)$ versus frequency $\omega/2\pi$ in a system of neurons on a square lattice of linear size $L = 128$ with shortcuts, obtained from the stationary MC time series of $q(t)$. In the system the number of coupled neighbors is chosen as $k_0 = 8$, with the number $N_{\rm sc}$ of shortcuts taking several values ranging from 22 000 to 47 000. It is observed that the power spectrum for $N_{\rm sc} = 22\,000$ or

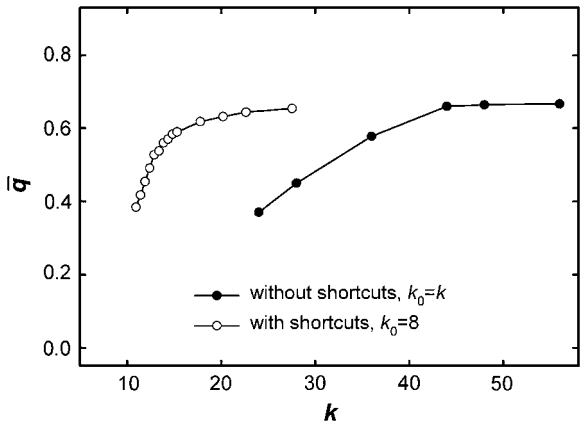

Figure 1. The average value of the Mattis-state order parameter $\bar{q}$ versus the average number k of connections per neuron. Data are obtained from MC simulations, for which the number of connections per neuron corresponds just to the number of neighboring coupled neurons, i.e., $k = k_0$ (solid circles). Also shown are the data when shortcuts are present with $k_0 = 8$ (empty circles). There are a total of $N = L^2 = 4096$ neurons with the time ratio $a = 0.5$, on a square lattice of size $L = 64$ at temperature $T = 0.1$. Lines are merely guides to the eye.

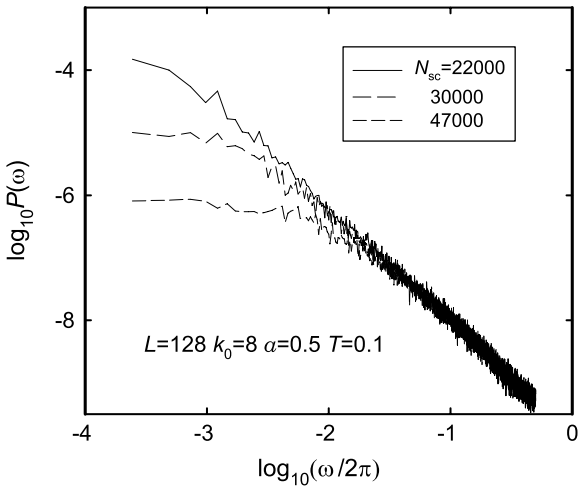

Figure 2. The power spectrum $P(\omega)$ versus frequency $\omega/2\pi$, obtained from stationary MC time series of the order parameter for several values of N_{sc} as shown in the legend. The neurons are placed on a square lattice of $L = 128$, with the number of coupled neighbors given by $k_0 = 8$.

$k = 10.7$ exhibits apparently power-law behavior: $P(\omega) \propto \omega^{-\gamma}$ with the exponent $\gamma = 1.8$ over a wide range of the frequency $\omega/2\pi$. For a larger value of N_{sc} or k, the power spectrum gradually deviates from the power law below a certain frequency, resulting in a shrink of the power-law region. We recall that for large N_{sc} the system has already approached the ordered state and fluctuations are relatively small. In the mean time, for $k = 10.7$, the system is near the region in which the transition from disordered to ordered state takes place, where large fluctuations are present. This type of behavior is also observed in the dynamic failure model, where both the phase transition and SOC may come into play [17].

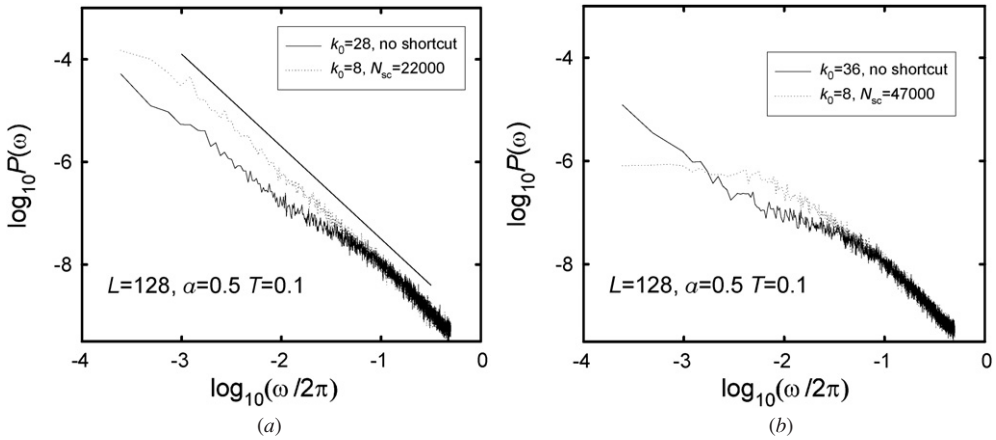

Figure 3. Comparison of the power spectra for a system on a square lattice of $L = 128$ in the absence/presence of shortcuts. (*a*) $k_0 = 28$ without shortcuts and $k_0 = 8$ with the number of shortcuts $N_{sc} = 22\,000$. The other parameters are the same as those in figure 1. Both sets of data correspond essentially to the same value of the order parameter $\bar{q} = 0.21$. Also plotted for comparison is a straight line of slope -1.8. (*b*) $k_0 = 36$ with $N_{sc} = 0$ and $k_0 = 8$ with $N_{sc} = 47000$. Both correspond to $\bar{q} = 0.56$.

The power spectra for systems without shortcuts exhibit somewhat different features. Compared in figure 3(*a*) are the power spectra for two systems, one without shortcuts for $k_0 = 28$ (solid line) and the other with shortcuts for $k_0 = 8$ and $N_{sc} = 22\,000$ (dotted line). With other parameters the same as those in figure 2, both systems have essentially the same value of the order parameter, $\bar{q} = 0.21$. Note that the power spectrum for the system without shortcuts displays an inflection point, unlike that for the system with shortcuts. Such features persist for other values of connectivity, as shown in figure 3(*b*) for a higher value of the order parameter. It is thus concluded that qualitative behavior of the power spectrum depends on the connectivity as well as how neurons are connected.

In view of the likely connection between spatial and temporal correlations, we expect to observe power-law behavior of spatial correlations, e.g., power-law distribution of cluster sizes, in the regime where power-law behavior of the power spectrum emerges. We therefore measure the size s of each cluster of 'memory-unmatched neurons', i.e., those neurons in state s_i with $s_i\sigma_i = -1$. By a cluster, we mean a group of neurons connected as neighbors in the same state. Figure 4 presents the obtained cluster size distribution $D(s)$ in systems with/without shortcuts at stationarity, for (*a*) $\bar{q} = 0.21$ and (*b*) $\bar{q} = 0.56$. As observed in figure 4(*a*), the size distribution in the system with shortcuts (open circles) fits in the power law $D(s) \sim s^{-\alpha}$ in the wider range than the system without shortcuts (filled circles). Also shown are the least-square fit lines, corresponding to the exponent $\alpha = 1.7$ (dotted line) and $\alpha = 2.0$ (solid line), respectively. It is observed that the size distribution does not fit well in the power law in the full range of s, whenever the corresponding power spectrum deviates from the power-law behavior, namely, whenever $P(\omega)$ in figure 3 bends considerably; this is manifested in figure 4(*b*), regardless of the presence of shortcuts. Further, for systems without shortcuts, it is observed that the cluster size distribution $D(s)$ also has an inflection point just like the power spectrum $P(\omega)$, again revealing the connection between spatial and temporal correlations.

Note that the results shown in figures 3 and 4 represent averages over more than 20 configurations and the inflection point always appears in data for systems without shortcuts.

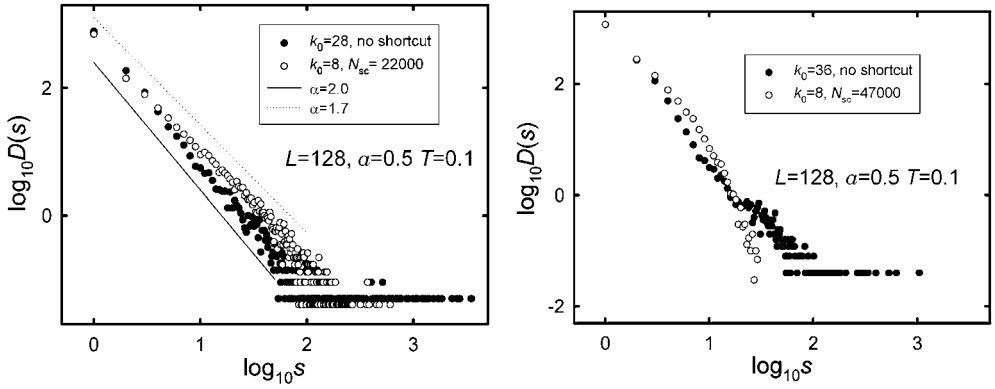

Figure 4. Cluster size distribution of memory-unmatched neurons for the data in (*a*) figure 3(*a*) and (*b*) figure 3(*b*). Straight lines in (*a*) have the slopes −2.0 and −1.7, as indicated in the legend.

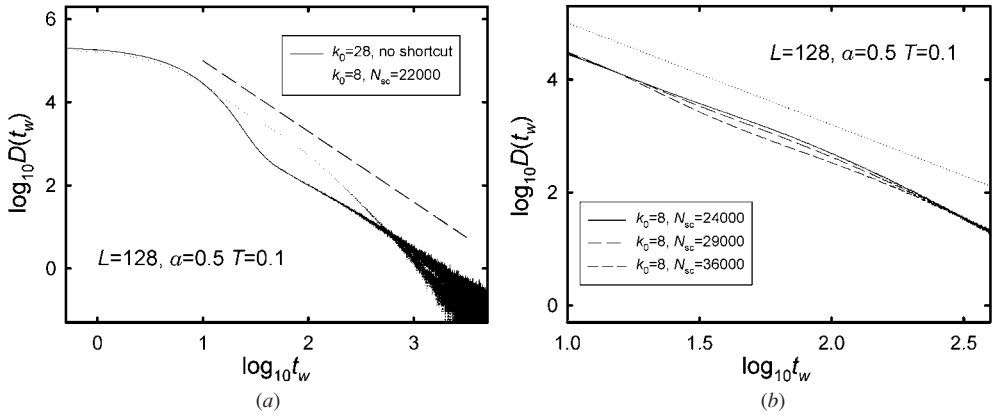

Figure 5. (*a*) Waiting time distribution of resting neurons for the data in figure 3(*a*). The broken line has the slope −1.7. (*b*) Waiting time distribution of resting neurons in networks with the number N_{sc} of shortcuts given in the legend. The dotted line corresponds to the exponent $\beta = 1.8$.

Although the physical meaning of the inflection point is not clear, the connection between spatial and temporal correlations presumably reflects the fact that events involving larger clusters occur rarely, i.e., in lower frequencies while those involving smaller clusters occur more frequently. Here the presence of shortcuts in the network would increase the correlation length of neuronal sites. It is likely that as the correlation length grows larger, so does the ranges of the power-law behaviors of the power spectrum and of the cluster size distribution. As a result, the frequency or the cluster size, at which the power spectrum or the distribution deviates from the power-law behavior, tends to shift to smaller values. This appears to explain why the inflection point is observed only in a system without shortcuts, where the correlation length is relatively small.

Finally, we consider the wait time t_w, defined as the time elapse for a resting neuron to wait for the next firing, and show in figure 5(*a*) the wait-time distribution $D(t_w)$, obtained for the same parameters as those in figure 3(*a*). It is observed that $D(t_w)$ does not fit well in the

power law for all t_w larger than the relaxation time $\tau = 5$, again displaying an inflection point in the absence of shortcuts. As the number of shortcuts is increased to a moderate amount, figure 5(*b*) shows that the distribution tends to fit better in the power law, $D(t_w) \sim t_w^{-\beta}$. Here the dotted line, plotted for comparison, corresponds to the exponent $\beta = 1.8$, which is consistent with observations in central nerve systems and cortex neurons [1, 3]. It is thus suggested that the system with shortcuts exhibits behavior following a power law more closely than that without shortcuts; this apparently supports the small-world architecture in the nervous system, with regard to the power-law behavior.

4. Summary

We have performed extensive Monte Carlo calculations on the dynamic model for neural networks, focusing on the effects of connectivity, i.e., number of coupled neurons. For this purpose, the neurons are placed on a two-dimensional lattice and the connectivity is varied in two ways: (i) by increasing the nearest neighbors and (ii) by introducing shortcuts in the network.

It has been observed that the Mattis-state order parameter, measuring the memory retrieval, grows gradually as the average number of connections (or coupled neurons) is increased. This effect becomes more pronounced when shortcuts are introduced in the network. The power spectrum of the order parameter at stationarity has also been computed to exhibit behavior depending on how the average number of connections is increased. Further, the power spectrum has been found to have correlations with the cluster size distribution of memory-unmatched sites. Among others, power-law behavior is observed both in the power spectrum and in the cluster size distribution, mostly of the system with shortcuts near the transition region where the network begins to order. The waiting time distribution has also been considered and found to follow roughly a power law in the presence of shortcuts. These results for the power-law behavior of the system with shortcuts are apparently consistent with the small-world architecture in nervous systems exhibiting power-law behavior.

Acknowledgments

One of us (MYC) thanks D Ham for hospitality during his stay at Harvard University, where part of this work was carried out. This work was supported in part by 2008 Research Fund of University of Ulsan.

References

[1] Gisiger T 2001 *Biol. Rev.* **76** 161
[2] Pritchard W S 1992 *Int. J. Neurosci.* **66** 119
Linkenkaer-Hansen K, Nikouline V V, Palva J M and Ilmoniemi R J 2001 *J. Neurosci.* **21** 1370
Beggs J and Plenz D 2003 *J. Neurosci.* **23** 11167
Freeman W J, Holms M D, West G A and Vanhatalo S 2006 *Clin. Neurophysiol.* **117** 1228
[3] Papa A R R and Da Silva L 1997 *Theory Biosci.* **116** 321
[4] See, for example, Christensen K and Moloney N R 2005 *Complexity and Criticality* (London: Imperial College Press)
[5] Bak P, Tang C and Wiesenfeld K 1987 *Phys. Rev. Lett.* **59** 381
Bak P, Tang C and Wiesenfeld K 1988 *Phys. Rev.* A **38** 364
[6] Bak P and Tang C 1989 *J. Geophys. Res.* **94** 15635
Ito K 1991 *Phys. Rev.* E **52** 3232
Drossel B and Schwbl F 1992 *Phys. Rev. Lett.* **69** 1629
Bak P and Sneppen K 1993 *Phys. Rev. Lett.* **71** 4083

[7] Sporns O, Tononi G and Edelman G M 2000 *Cereb. Cortex* **10** 127
Laughlin S B and Sejnowski T J 2003 *Science* **301** 1870
Chialvo D R 2004 *Physica* A **340** 756
[8] Roerig B and Chen B 2002 *Cereb. Cortex* **12** 187
Roerig B, Chen B and Kao J P Y 2003 *Cereb. Cortex* **13** 350
[9] Watts D J and Strogatz S H 1998 *Nature* **393** 440
Watts D J 1999 *Small Worlds* (Princeton: Princeton University Press)
Watts D J 1999 *Science* **284** 79
[10] Bohland J W and Minai A A 2001 *Neurocomputing* **38–40** 489
[11] de Arcangelis L, Perrone-Capano C and Herrmann H J 2006 *Phys. Rev. Lett.* **96** 028107
Pellegrini G L, de Arcangelis L, Herrmann H J and Perrone-Capano C 2007 *Phys. Rev.* E **76** 016107
[12] Choi M Y 1988 *Phys. Rev. Lett.* **61** 2809
Choi M Y and Choi M 1990 *Phys. Rev.* A **41** 7062
[13] Hebb D O 1949 *The Organisation of Behaviour* (New York: Wiley)
[14] Little W A 1974 *Math. Biosci.* **19** 101
Little W A and Shaw G A 1978 *Math. Biosci.* **39** 281
[15] Hopfield J J 1982 *Proc. Natl. Acad. Sci. USA* **79** 2554
[16] Yoon B-G, Choi J and Choi M Y 2008 *J. Phys. A: Math. Theor.* **41** 385102
[17] Jo J, Kang H, Choi M Y, Choi J and Yoon B-G 2008 *J. Phys. A: Math. Theor.* **41** 145101
[18] Yoon B-G, Choi J and Choi M Y 2005 *J. Korean Phys. Soc.* **47** 1053